ELSEVIER

Ceramics International 31 (2005) 411–415

CERAMICS
INTERNATIONAL

www.elsevier.com/locate/ceramint

Photoluminescence properties of spark-processed CuO

Sung-Sik Chang[a,*], Hyung-Jik Lee[a], Hye Jeong Park[b]

[a]*Department of Ceramic Engineering, Kangnung National University, Kangwondo 210-702, South Korea*
[b]*Department of Natural Science, Hankuk University of Foreign Studies, Seoul 130-791, South Korea*

Received 6 February 2004; received in revised form 27 March 2004; accepted 25 May 2004

Abstract

This paper reports the preparation of photoluminescing porous CuO using spark discharge in ambient air. The photoluminescence (PL) characteristics of spark processed CuO (sp-CuO) have been studied at various temperatures. Further studies of scanning electron microscopy (SEM) and X-ray photoelectron spectroscopy (XPS) have been performed. Visible light emission with peaks at around 400 and 570 nm is obtained from CuO. In addition to the visible light emission peaks at around 400 and 570 nm of bulk CuO, the photoluminescence studies of sp-CuO at room temperature and low temperature reveal two additional emission peaks at around 470 and 505 nm. XPS studies show that the slightly higher binding energy shift (Cu) and a broader peak which indicates an increase of multiple oxidation state. The newly detected emission bands of sp-CuO compared to the bulk CuO is associated with defect states within the emission peaks of CuO.

Keywords: Photoluminescence; Spark-processing; CuO; XPS

1. Introduction

The intense luminescence from spark processed materials has been studied mainly for Si [1], and to a smaller degree for other semiconductors such as Ge, GaAs [2,3], GaP [4], and semimetals [5]. When compared with the electrochemical etching method which is extensively used in preparation of porous silicon; a potentially desirable feature of spark processing is that it is a non-toxic, dry process that could be used to prepare various photoluminescing materials at ease, and avoid the complexities of the chemical anodization which results in complicated chemical structures. The spark processing transforms a crystalline Si into a mixture of highly porous silicon dioxide and nano-scale Si particles with nitrogen incorporated in the structure [6]. Spark-processed materials display fast decays in nanoseconds or faster and show stability with respect to peak wavelength and peak intensity against UV laser radiation, high temperatures up to at least 1000 °C, and etching in buffered hydrofluoric (HF) acid up to 30 min [7].

Various experimental approaches on spark-processed materials are attempted to limit the number of possible PL mechanisms [8]. Nevertheless, the origins of these luminescence bands obtained from spark processed materials are casually assigned as quantum size related luminescence [9] and/or formation of a particular molecular cluster or defect during spark processing [5]. Spark processed materials which exhibit substantial PL after spark-processing consists of stable oxide layers, which possess band gaps wide enough to host defect states in the optical transition range.

The present paper extends our previous studies to find out if subjection of a metal oxide (especially CuO) to spark processing would yield any PL. Further, the characteristics of luminescence properties of sp-CuO, especially on the temperature dependence, scanning electron microscopy (SEM), X-ray diffraction (XRD) and X-ray photoelectron spectroscopy (XPS) measurements are performed and the possible mechanisms of newly detected luminescence bands are discussed.

---

* Corresponding author. Tel.: +82 33 640 2366; fax: +82 33 640 2244.
E-mail address: chang@knusun.kangnung.ac.kr (S.-S. Chang).

0272-8842/$30.00 © 2004 Elsevier Ltd and Techna Group S.r.l. All rights reserved.
doi:10.1016/j.ceramint.2004.05.027

2. Experimental

CuO powders (Aldrich Chemical Co., 99.99% purity) were pressed into cylindrical pellets (1 mm thick and 10 mm in diameter) at 1000 psi. Subsequently, the pellets were sintered at 1200 °C for 1 h under ultra high purity oxygen atmosphere. A high voltage (10^4 V), low average current (several mA) and high frequency (10^4 Hz) were applied for 30 min, as described earlier [2]. The spark gap distance was 1 mm. The spark discharge occurred in ambience between a tungsten wire (1 mm in diameter) as anode and the above-mentioned sintered CuO pellet as cathode.

The PL equipment consists of a He–Cd laser, 50-mm collection optics, 0.5-m scanning grating monochromator and an air-cooled GaAs photomultiplier. Parasitic plasma emission from the laser was filtered by the use of 325 laser line interference filter. A long-pass filter was inserted after the sample to block any scattered laser light. The temperature-dependent PL measurements were taken by placing the sample in the cold finger of a closed-cycle He refrigerator that allows setting between 20 and 300 K. X-ray photoelectron spectroscopy analysis has been performed to interpret the luminescence mechanism involving spark processed CuO.

3. Results and discussion

Fig. 1 shows the typical morphology of a sp-CuO. Visual inspection of spark affected areas reveals damaged oblate features. A similar shape and morphology are also observed for sp-Si [1]. It is interesting to note that the spark affected region exhibits coalescence and small fragmented granules as can be seen in Fig. 1(b).

X-ray diffraction measurements are performed on sintered CuO as well as sp-CuO and the results are depicted in Fig. 2. The diffraction peaks of sintered CuO display a good agreement with JCPDS card of CuO (JCPDS 41-0254). No characteristic peaks of impurities are observed from CuO. The calculated lattice constants and unit cell volume of sintered monoclinic CuO are $a = 4.690 \pm 0.002$ Å, $b = 3.419 \pm 0.002$ Å and $c = 5.131 \pm 0.002$ Å, and 81.13 Å^3, respectively, and are agreed to the values obtained from JCPDS. The diffraction peaks of sp-CuO exhibit the characteristics of CuO with somewhat reduced diffraction peak intensities. Further, a small contraction of lattice constants (a = 4.685 Å, b = 3.415 Å, and c = 5.125 Å) are observed, and resulted in decrease of the unit cell volume (80.89 Å^3). It seems that the decrease in lattice constants and unit cell volume of sp-CuO is associated with the thermal stress upon cooling from vigorous spark event. It is quite interesting that the similar decrease in lattice constant and unit cell volume is also observed for spark processed Sn [10].

Fig. 3 displays PL spectra of (a) CuO and (b) sp-CuO measured at room temperature. The PL intensities of these

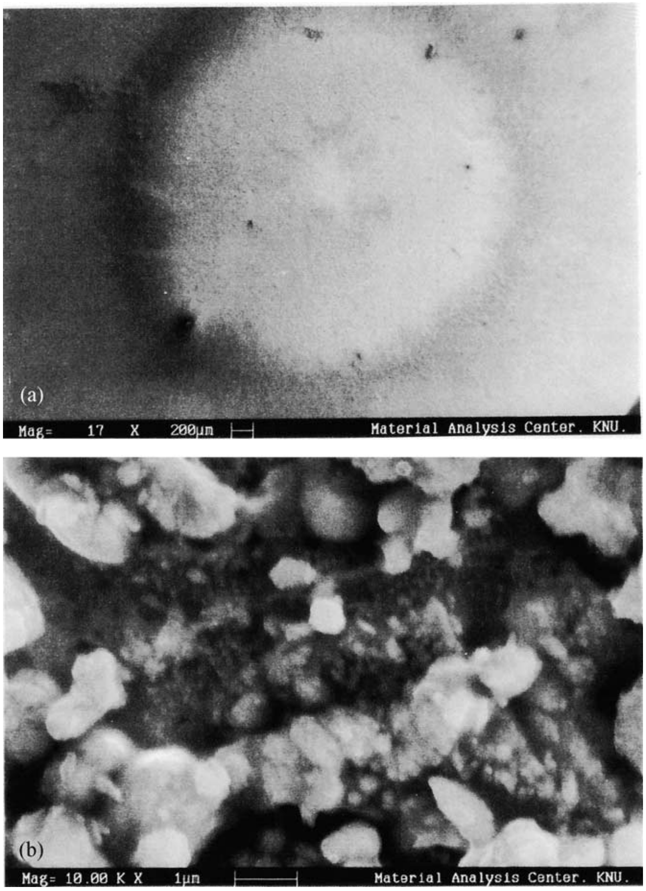

Fig. 1. Plan view scanning electron microscopes of spark-processed CuO (a) showing overall spark-affected area and center area with high magnification (b).

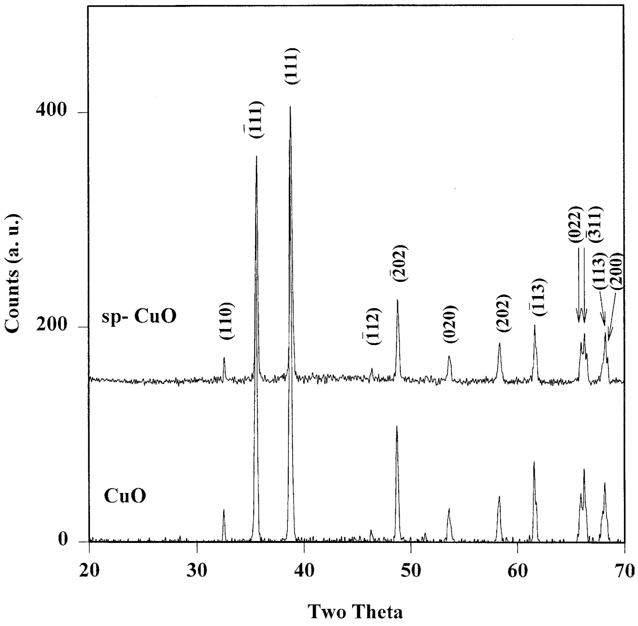

Fig. 2. X-ray diffraction patterns of sintered CuO and sp-CuO.

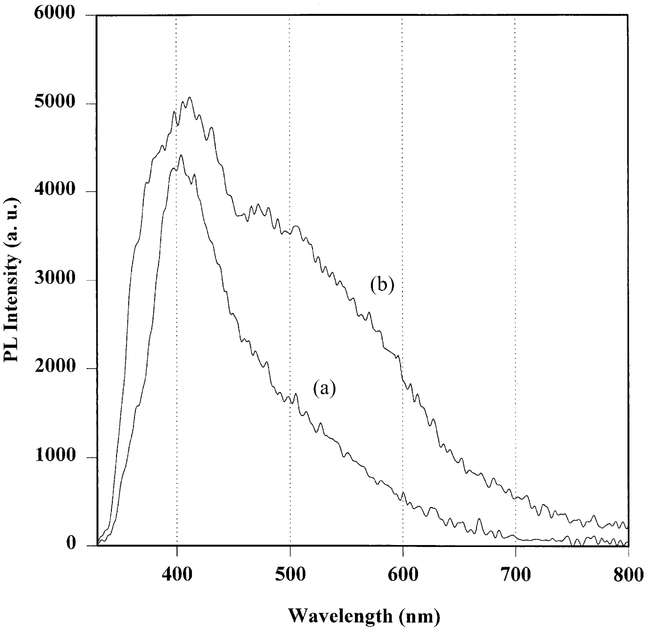

Fig. 3. Room temperature photoluminescence spectra of (a) CuO and (b) sp-CuO excited by 325 nm line of He–Cd laser.

two spectra are quite comparable to each other. The sintered CuO exhibits a broad violet luminescence band around 403 nm (3.08 eV) with a broad tail in the green spectral region. sp-CuO also shows the similarly broad luminescence band with a broad pronounced shoulder peak in the blue–green spectral region of sintered CuO.

Fig. 4 shows various PL spectra measured at some selected temperature to delineate possible similarities and differences between CuO and sp-CuO. The measurement temperatures are indicated in the figure. The sintered CuO exhibits an additional luminescence band at 576 nm (2.18 eV) when the measurement temperatures are cooled below 100 K. Sp-CuO also reveals the 576 nm luminescence peak. The PL intensity of this luminescence band is quite comparable to that of the violet luminescence band when the temperature is cooled down to 20 K. However, the most dramatic change of the luminescence spectra of sp-CuO which are measured at low temperatures, is the appearance of two additional narrow shoulder peaks at 474 (2.62 eV) and 508 nm (2.44 eV). The detailed temperature dependence of PL peaks in terms of PL peak energies, full width at half maximum (FWHM), and PL intensities of sp-CuO are presented in Fig. 5. The luminescence peaks of 2.18, 2.44, 2.62, and 3.15 eV are depicted as ○, □, △, and ▽, respectively. All of the observed luminescence bands display almost constant luminescence peak energies. One could detect two additional shoulder peaks at 2.62 and 2.44 eV with a similar FWHM value (about 0.18 eV) when the measurement temperatures are increased up to 225 °C. The FWHM of 3.15 eV luminescence band is increased slightly with increasing temperature. The temperature dependence of PL intensities of 2.18, 2.44, and 2.62 eV

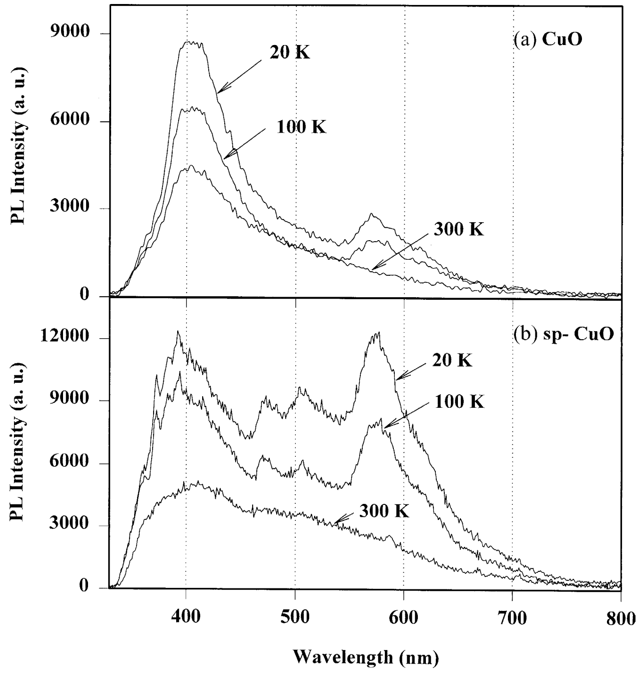

Fig. 4. Temperature dependence of PL spectra of (a) CuO and (b) sp-CuO. Measurement temperatures are indicated in the figure.

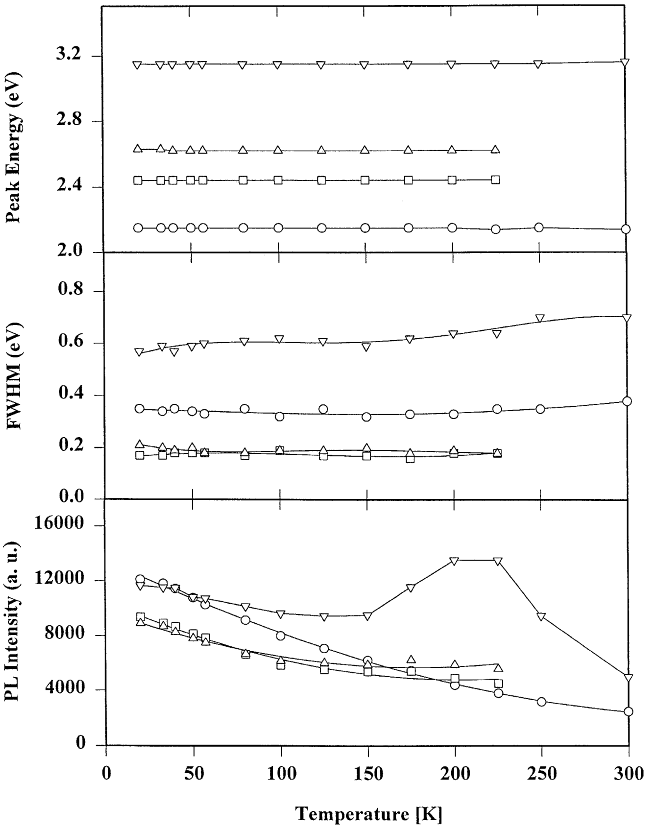

Fig. 5. Temperature dependence of photoluminescence peak energies, full width at half maximum (FWHM), and PL intensities. The luminescence peaks of 2.18. 2.44, 2.62, and 3.15 eV are depicted as ○, □, △, and ▽, respectively.

luminescence bands shows continuous decrease with increasing temperature, as can be seen in Fig. 5. The PL intensity of 3.15 eV tends to decrease with increasing temperature. This decrease in PL intensity does not seem to occur steadily, however. Instead, the peak of PL intensity is observed at 225 K, as can be seen in Fig. 5. No blue shift upon cooling of the newly detected 2.62 and 2.44 eV luminescence band from sp-CuO clearly shows that no quantum size effects can be inferred.

In order to investigate the chemical species formed during the spark process, XPS profiles were obtained by scanning the O 1s and Cu 2p regions for sp-CuO and a reference CuO sample. The results are depicted in Fig. 6. As shown in Fig. 6, the O 1s core-level spectrum of reference CuO is composed of two O 1s peaks, i.e. peak at 529.7, which is in agreement with O^{2-} in CuO, and shoulder peak at 532.1 eV. For sp-CuO, the shoulder peak of O 1s becomes a comparable with O 1s peak (529.7 eV) of CuO. It is interesting to note that the binding energy of O 1s displays a slightly higher energy shift and broader spectra, which indicates a multiple oxidation state probably formed during spark processing. The sintered CuO displays the broad Cu $2p_{3/2}$ peaking at 932.5, the shoulder peak at 934.5 eV, the broad Cu $2p_{1/2}$ peaking at 952.5 and shoulder peak at 954.5 eV. The maximal peak energy corresponds to the Cu_2O and the shoulder peak corresponds to the CuO. These peaks are accompanied by shake-up satellite peaks approximately 9 eV higher in binding energy than that of the main peak, as shown in Fig. 6. It is reported that the high temperature annealing transforms CuO to Cu_2O [11]. Therefore, XPS studies of Cu 2p peaks in sintered CuO display a mixture of CuO and Cu_2O. It is interesting to note that sp-CuO shows a slight high binding energy shift of about 0.6 eV with an increase of FWHM of Cu 2p peaks. The optical band gap of CuO is not well known due to no transparent gap in the visible and near infrared and most data are obtained for thin films. The reported band gap of Cu_2O, which is calculated from optical absorption and photoluminescence measurement, is 571 nm (2.17 eV) [12]. The existence of Cu_2O, as evidenced by XPS analysis and luminescence peak at 570 nm observed below 225 K for both sintered CuO and sp-CuO might result from the reported band gap of Cu_2O. Particular interest is given to the newly detected emission bands, namely at 474 and 508 nm from sp-CuO. According to the report of Jana et al. [13], a metastable cuprous oxide (Cu_2O) displays an excitonic series of three emission peaks at 408 nm (3.04 eV), 460 nm (2.7 eV), and 524 nm (2.37 eV) with a 265 nm (4.68) excitation. However, the emission band at 408 and 460 nm disappear and other emission bands appear, which are centered near 590 nm (2.10 eV) and 630 nm (1.97 eV), when the cuprous oxide are excited at 350 and 400 nm (3.1 eV). Therefore, a newly detected emission band from sp-CuO seems to be unrelated to the excitonic emission bands from Cu_2O. It is generally observed that the high-energy emission bands are detected for spark-processed materials such as semiconductor and semi-metals compared to unsparked materials. The spark treatment of materials produces randomly oriented nanosized crystallites surrounded by amorphous oxide. Amorphous oxide occupies most of the volume of the spark-processed material with a small concentration of N incorporation into the spark-processed material. The proposed mechanisms consider predominantly radiative recombination of quantum confined electron/hole pair in nanocrystals or formation of particular molecular cluster or defect in oxide structure during spark processing [5]. However, the newly detected emission bands at 474 and 508 nm of sp-CuO display no shift of peak energy upon cooling, as shown in Fig. 5. Thus, no quantum size effects can be inferred from sp-CuO. Spark processed materials which exhibit substantial PL consist of stable oxide layer, which possess band-gaps wide enough to host defect states in the optical transition range. Thus, the metal oxides provide the framework for the band gap where spark-created defect centers are contained. A recombination between donor defect centers and acceptor defect centers would yield the observed emission peaks. Recent electron paramagnetic resonance (EPR) studies of spark-processed Si show defect centers in the excess of 10^{19} cm^{-3} [14]. Further, the multiple oxidation states in O 1s and Cu 2p spectra of sp-

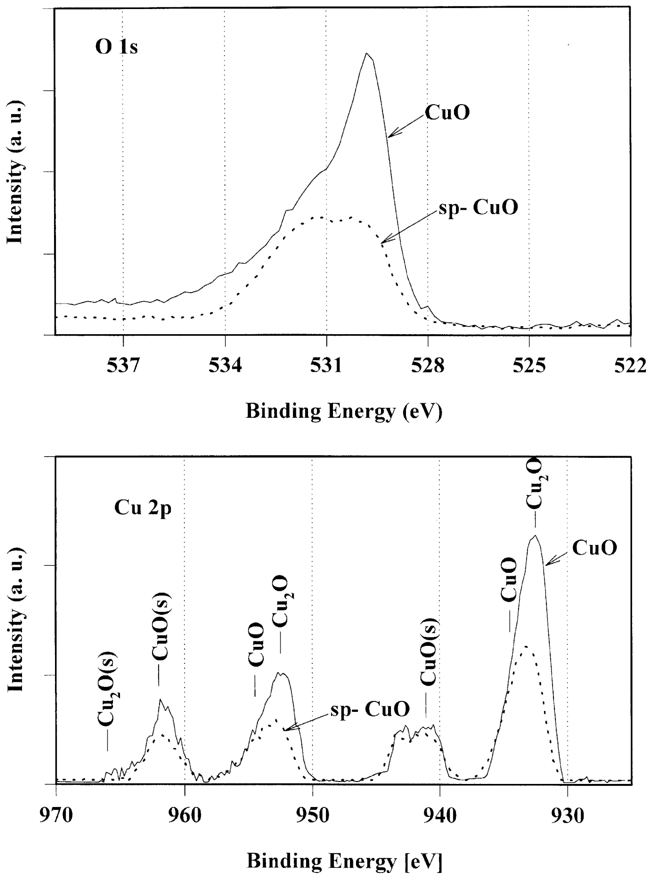

Fig. 6. X-ray photoelectron spectra of the O 1s and Cu 2p regions for CuO and sp-CuO.

CuO, as shown in Fig. 6, support the defect-related luminescence within oxide layer.

4. Conclusion

Spark processing of CuO yields novel PL emission bands, i.e. 474 and 508 nm. The experimental results such as low temperature PL measurements and XPS analysis reveal that the origin of the new luminescence band observed from sp-CuO may be due to the defect-related luminescence formed during spark processing, but not due to a quantum confinement.

Acknowledgement

This work was supported by grant R05-2002-000-00114-0 from the Basic Research Program of the Korea Science & Engineering Foundation.

References

[1] R.E. Hummel, S.-S. Chang, Appl. Phys. Lett. 61 (1992) 1965.
[2] M.H. Ludwig, R.E. Hummel, S.-S. Chang, J. Vac. Sci. Technol. B12 (1994) 3023.
[3] S.-S. Chang, R.E. Hummel, J. Lumin. 86 (2000) 33.
[4] S.-S. Chang, W. Gao, Mater. Sci. Eng. B85 (2001) 1.
[5] M.E. Stora, R.E. Hummel, J. Phys. Chem. Solids 63 (2002) 1867.
[6] M. Ludwig, Crit. Rev. Solid State Mater. Sci. 21 (1996) 255.
[7] S.-S. Chang, Dissertation, University of Florida, 1994.
[8] J.G. Polihronov, M. Hedstrom, R.E. Hummel, H.-P. Cheng, J. Lumin. 96 (2002) 119.
[9] R.H. Hummel, A. Morrone, M.H. Ludwig, S.-S. Chang, Appl. Phys. Lett. 63 (1993) 2771.
[10] S.-S. Chang, D.K. Park, Mater. Sci. Eng. B95 (2002) 55.
[11] S.Y. Lee, N. Mettlach, N. Nguyen, Y.M. Sun, J.M. White, Appl. Surf. Sci. 206 (2002) 102.
[12] S.C. Ray, Sol. Energy Mater. Sol. Cells 68 (2001) 307.
[13] S. Jana, P.K. Biswas, Mater. Lett. 32 (1997) 263.
[14] S.-S. Chang, G.A. Bowmaker, Mater. Sci. Eng. B95 (2002) 290.